Journal of Thrombosis and Haemostasis, **12**: 1182–1192 DOI: 10.1111/jth.12602

ORIGINAL ARTICLE

Particle size distribution of exosomes and microvesicles determined by transmission electron microscopy, flow cytometry, nanoparticle tracking analysis, and resistive pulse sensing

E. VAN DER POL,*† F. A. W. COUMANS,*† A. E. GROOTEMAAT,* C. GARDINER,‡ I. L. SARGENT,‡ P. HARRISON,§ A. STURK,* T. G. VAN LEEUWEN† and R. NIEUWLAND*

**Laboratory of Experimental Clinical Chemistry, Academic Medical Center, University of Amsterdam; †Biomedical Engineering and Physics, Academic Medical Center, University of Amsterdam, Amsterdam, the Netherlands; ‡Nuffield Department of Obstetrics and Gynaecology, John Radcliffe Hospital, Oxford; and §School of Immunity and Infection, University of Birmingham Medical School, Birmingham, UK*

To cite this article: van der Pol E, Coumans FAW, Grootemaat AE, Gardiner C, Sargent IL, Harrison P, Sturk A, van Leeuwen TG, Nieuwland R. Particle size distribution of exosomes and microvesicles determined by transmission electron microscopy, flow cytometry, nanoparticle tracking analysis, and resistive pulse sensing. *J Thromb Haemost* 2014; **12**: 1182–92.

Summary. *Background:* Enumeration of extracellular vesicles has clinical potential as a biomarker for disease. In biological samples, the smallest and largest vesicles typically differ 25-fold in size, 300 000-fold in concentration, 20 000-fold in volume, and 10 000 000-fold in scattered light. Because of this heterogeneity, the currently employed techniques detect concentrations ranging from 10^4 to 10^{12} vesicles mL^{-1}. *Objectives:* To investigate whether the large variation in the detected concentration of vesicles is caused by the minimum detectable vesicle size of five widely used techniques. *Methods:* The size and concentration of vesicles and reference beads were measured with transmission electron microscopy (TEM), a conventional flow cytometer, a flow cytometer dedicated to detecting submicrometer particles, nanoparticle tracking analysis (NTA), and resistive pulse sensing (RPS). *Results:* Each technique gave a different size distribution and a different concentration for the same vesicle sample. *Conclusion:* Differences between the detected vesicle concentrations are primarily caused by differences between the minimum detectable vesicle sizes. The minimum detectable vesicle sizes were 70–90 nm for NTA, 70–100 nm for RPS, 150–190 nm for dedicated flow cytometry, and 270–600 nm for conventional flow cytometry. TEM could detect the smallest vesicles present, albeit after adhesion on a surface. Dedicated flow cytometry was most accurate in determining the size of reference beads, but is expected to be less accurate on vesicles, owing to heterogeneity of the refractive index of vesicles. Nevertheless, dedicated flow cytometry is relatively fast and allows multiplex fluorescence detection, making it most applicable to clinical research.

Keywords: cell-derived microparticles; exosomes; optical devices; reference standards; secretory vesicles.

Correspondence: Edwin van der Pol, Biomedical Engineering and Physics, Academic Medical Center, University of Amsterdam, Meibergdreef 9, PO Box 22660, 1100 DD, Amsterdam, the Netherlands.
Tel.: +31 20 5664386; fax: +31 20 5669569.
E-mail: e.vanderpol@amc.uva.nl

Received 21 November 2013
Manuscript handled by: P. H. Reitsma
Final decision: P. H. Reitsma, 25 April 2014

Introduction

Extracellular vesicles, such as exosomes and microvesicles, are released by cells into their environment as submicrometer particles enclosed by a phospholipid bilayer [1]. These vesicles contribute to many homeostatic processes, e.g. coagulation and inflammation [2–4], and therefore have potential clinical applications [5–8]. Unfortunately, most single vesicles are below the detection range of many techniques, owing to their small size and low refractive index [9,10], leading to misinterpretation of data and reported concentrations ranging from 10^4 to 10^{12} vesicles mL^{-1} in plasma [9–15].

In 2010, we reviewed the theoretical performance of 13 methods to determine the particle size distribution (PSD) of vesicles [9]. The PSD describes the concentration as a function of size, and defines which vesicle types are measured [4]. Unexpectedly, our simulations predicted that each method would obtain a different PSD, thereby hampering data interpretation, data comparison, and standardization.

Table 1 Catalog numbers, diameters and concentrations of the subpopulations of polystyrene reference beads as determined by five methods

Catalog number	3050A	3100A	3200A	3400A	3600A
Diameter (nm)					
TEM	46 ± 7	102 ± 5	203 ± 5	400 ± 7	596 ± 8
Conventional flow cytometer	–	–	209 ± 8	427 ± 33	592 ± 20
Dedicated flow cytometer	–	105 ± 4	193 ± 4	399 ± 6	589 ± 7
NTA	49 ± 11	93 ± 21	189 ± 23	380 ± 64	607 ± 27
RPS	–	104 ± 10	200 ± 10	418 ± 31	623 ± 36
Concentration (beads mL^{-1})					
Prepared	2.0×10^9	1.0×10^9	1.0×10^8	1.0×10^7	1.0×10^6
Conventional flow cytometer			1.0×10^8	1.0×10^7	0.7×10^6
Dedicated flow cytometer		0.5×10^9	0.8×10^8	0.8×10^7	0.9×10^6
NTA	0.1×10^9	1.0×10^9	1.2×10^8	2.5×10^7	1.0×10^6
RPS		1.1×10^9	1.2×10^8	1.0×10^7	1.0×10^6

NTA, nanoparticle tracking analysis; RPS, resistive pulse sensing; TEM, transmission electron microscopy. Diameter is expressed as mean ± standard deviation.

In this study, we performed an experimental evaluation of five of the 13 methods. We selected the most widely used methods capable of detecting single vesicles: transmission electron microscopy (TEM), a conventional flow cytometer, a flow cytometer dedicated to detecting submicrometer particles, nanoparticle tracking analysis (NTA), and resistive pulse sensing (RPS). The PSDs of a standard population of reference beads and a standard population of vesicles were measured with all methods.

Materials and methods

PSD

Throughout this article, we define 'size' as the diameter of a particle, and the PSD as the histogram of particle sizes, providing the mean number of particles per milliliter per 10-nm bin [16]. Data processing and representation were performed with ORIGINPRO (v8.0724; OriginLab Corporation, Northampton, MA, USA).

Reference beads

To create a reference sample with a known PSD, a mixture of traceable polystyrene beads (Nanosphere; Thermo Fisher, Waltham, MA, USA) was prepared in de-ionized water. RPS measurements require a conductive medium; therefore, the beads were suspended in electrolyte buffer (Izon, Christchurch, New Zealand). The size and concentration of the reference beads were selected to resemble those of previously reported vesicle PSDs [9,11–13,15,17]. Table 1 shows the size of the reference beads according to TEM data of the manufacturer. The concentration (beads mL^{-1}) was derived from the specifications. Figure 1A shows the PSD of the reference beads under the assumption that each subpopulation has a Gaussian distribution. The reference sample contained five subpopulations, among which larger beads have lower concentrations. The total concentration was 3.1×10^9 beads mL^{-1}. Prior to analysis, the reference sample was sonicated for 10 s and vortexed for 10 s. Table 2 lists the diameters of silica beads (Silica Oxide Size Standards [Corpuscular, Cold Spring, NY, USA]; Plain Silica [Kisker, Steinfurt, Germany]) used to calibrate the flow cytometers and NTA instrument.

Vesicle standard

As isolation of vesicles from blood is challenging [18], we selected urinary vesicles for our biological standard sample. Urine contains a relatively high concentration of vesicles with low contamination [9]. Urine from five healthy male individuals was collected, pooled, and centrifuged twice (8 × 50 mL, 10 min, 180 × *g*, 4 °C; and 20 min, 1550 × *g*) to remove cells. Cell-free urine aliquots (12 mL) were frozen in liquid nitrogen and stored at – 80 °C. Prior to analysis, samples were thawed on melting ice for 1 h, centrifuged (10 min, 1550 × *g*, 4 °C) to remove precipitated salts, and diluted in 0.2-μm-filtered (MilliPore, Billerica, MA, USA) phosphate-buffered saline.

TEM

Data from the manufacturer were used to create the PSD of reference beads by TEM. For analysis of the vesicle standard by TEM (CM-10; Philips, Eindhoven, The Netherlands), vesicles were prepared and analyzed as described in Data S1. To obtain the vesicle concentration, we multiplied the mean number of vesicles per surface area by the grid area, divided by the sample volume. Here, we assumed that all vesicles adhered to the grid and were distributed uniformly.

Conventional flow cytometry

A flow cytometer (FACSCalibur; BD, Franklin Lakes, NJ, USA) with a 15-mW 488-nm laser was used to detect

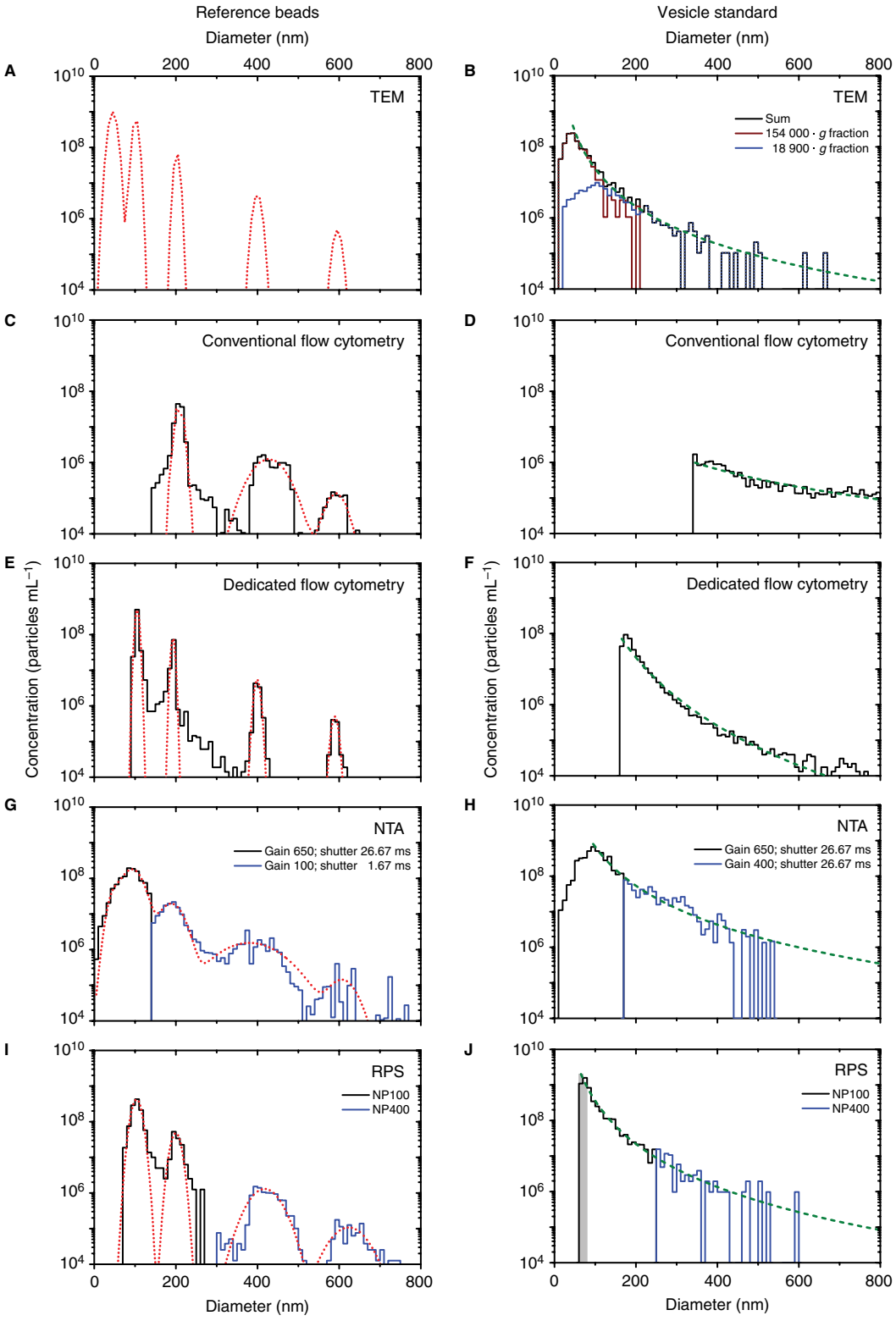

Fig. 1. Particle size distribution (PSD). Concentrations (on a logarithmic scale) of the reference beads (left) and the vesicle standard (right) detected by (A, B) transmission electron microscopy (TEM), (C, D) conventional flow cytometry, (E, F) dedicated flow cytometry, (G, H) nanoparticle tracking analysis (NTA) and (I, J) resistive pulse sensing (RPS) are shown. The bin width is 10 nm. PSDs of the reference beads (black line) were fitted by a sum of Gaussian functions (dotted red line). PSDs of the vesicle standard (black line) were fitted by a power-law function (dashed green line). The PSD of the reference beads determined by TEM is based on data from the manufacturer. PSDs given by NTA and RPS originate from two measurements with relatively high-sensitivity (black) and low-sensitivity (blue) settings.

Table 2 Manufacturers, catalog numbers and diameters of silica beads obtained by imaging at least 500 beads with transmission electron microscopy

Manufacturer	Catalog number	Diameter (nm)
Corpuscular	147020-10	105 ± 21
Kisker	Psi-0.2	206 ± 18
	Psi-0.4	391 ± 18
	Psi-0.6	577 ± 20
	Psi-0.8	772 ± 21
	Psi-1.0	918 ± 14

Diameter is expressed as mean ± standard deviation.

side-scattered light (SSC) for 10 min at a flow rate of ~ 60 μL min^{-1}. The detector settings are described in Data S1. To calculate the particle concentration, the flow rate was determined by weighting the sample volume aspirated during 10 min. To prevent swarm detection [15], the reference beads and vesicle standard were diluted 1000-fold (1.7×10^5 counts vs. 1.0×10^5 background counts) and 100-fold (2.6×10^5 counts vs. 1.5×10^5 background counts), respectively. The absence of swarm detection was confirmed by serial dilutions.

To relate SSC to a particle size, we calibrated the flow cytometer with beads of known size and refractive index. Figure 2A shows the SSC histogram of polystyrene beads. Figure 2B shows the SSC of polystyrene and silica beads vs. their size. The data were fitted by Mie theory, incorporating the size and refractive index of the beads and the optical configuration of the instrument [19]. Mie calculations were performed with the scripts of Mätzler [20] in MATLAB (v7.9.0.529). The solid curve in Fig. 2B was used to relate SSC to the size of the polystyrene reference beads with a refractive index of 1.61 [15]. The dashed curve in Fig. 2B was used to relate SSC to vesicle size, with the assumption that vesicles are spheres with a refractive index of 1.40, which was previously estimated [14] and corresponds to the refractive index of cells [21,22].

Dedicated flow cytometry

Throughout this article, we use 'dedicated flow cytometry' as a generic term for flow cytometers dedicated to detecting submicrometer particles. A flow cytometer (A50-Micro; Apogee, Hemel Hempstead, UK) with a 20-mW 488-nm laser was used to detect forward-scattered light (FSC) and SSC. The detector settings are described in Data S1. The sample volume injected by the internal microsyringe was used to calculate the concentration of particles. In total, 1.4×10^5 reference beads and 0.8×10^5 vesicles were analyzed. Analogously to our approach for conventional flow cytometry, we related FSC to the vesicle size by using beads and Mie theory, as illustrated for dedicated flow cytometry in Fig. 2C,D.

NTA

A dark-field microscope (NS500; Nanosight, Amesbury, UK) with a 45-mW 405-nm laser and an electron multiplying charge-coupled device (EMCCD) was used to determine the PSD by tracking the Brownian motion of single particles [12,23]. Measurements were performed with two dilutions and two detection settings to increase the effective size range, which is needed because light scattered from the smallest and the largest beads differs by five orders of magnitude, whereas the dynamic range of the EMCCD is only approximately three orders of magnitude. Consequently, settings suitable for detecting 46-nm beads would result in extreme saturation for 596-nm beads. Two dilutions are needed, because a 50-fold dilution is required to detect the smallest beads [23], but at this dilution the probability of detecting a 596-nm bead is < 0.5%.

Reference beads were analyzed with high-sensitivity settings (diluted 1 : 50; shutter, 26.67 ms; gain, 650; threshold, 22; 1.8×10^3 beads tracked) and low-sensitivity settings (undiluted; shutter, 1.67 ms; gain, 100; threshold, 10; 1.1×10^4 beads tracked). We multiplied the concentration as provided by the NTA software by the ratio between the expected and measured concentrations of calibration beads [23]. This concentration calibration was performed with 102-nm and 203-nm polystyrene beads with concentrations of 2×10^7 and 1×10^8 beads mL^{-1} for the high-sensitivity and low-sensitivity settings, respectively. The vesicle standard was analyzed with high-sensitivity settings (diluted 1 : 500; shutter, 26.67 ms; gain, 650; threshold, 19; 1.0×10^3 vesicles tracked) and low-sensitivity settings (diluted 1 : 100; shutter, 26.67 ms; gain, 400; threshold, 10; 1.1×10^3 vesicles tracked). Concentration calibration was performed with 105-nm and 206-nm silica beads with a concentration of 1×10^8 beads mL^{-1} for both the high-sensitivity and low-sensitivity settings [23], as the refractive indices of silica and vesicles are close.

Per sample, 20 videos of 30 s were captured at 22.0 °C and analyzed by NTA v2.3.0.17 (Nanosight), assuming a medium viscosity of 0.95 cP. To obtain the overall PSD $O(d)$, the PSDs obtained with high-sensitivity settings, $H(d)$, and low-sensitivity settings, $L(d)$, were combined at the size d_0, where the concentrations were similar [$H(d_0) \approx L(d_0)$, $O(d) = H(d)$ for all $d \leq d_0$; $O(d) = L(d)$ for all $d > d_0$].

RPS

RPS (qNano; Izon) determines the PSD from resistance pulses caused by particles moving through a pore. Measurements were performed with two pore sizes, for two reasons. First, for a single pore, the detectable size range is at best five-fold, whereas our smallest and largest reference beads differ 12-fold in size. Second, the analyzed

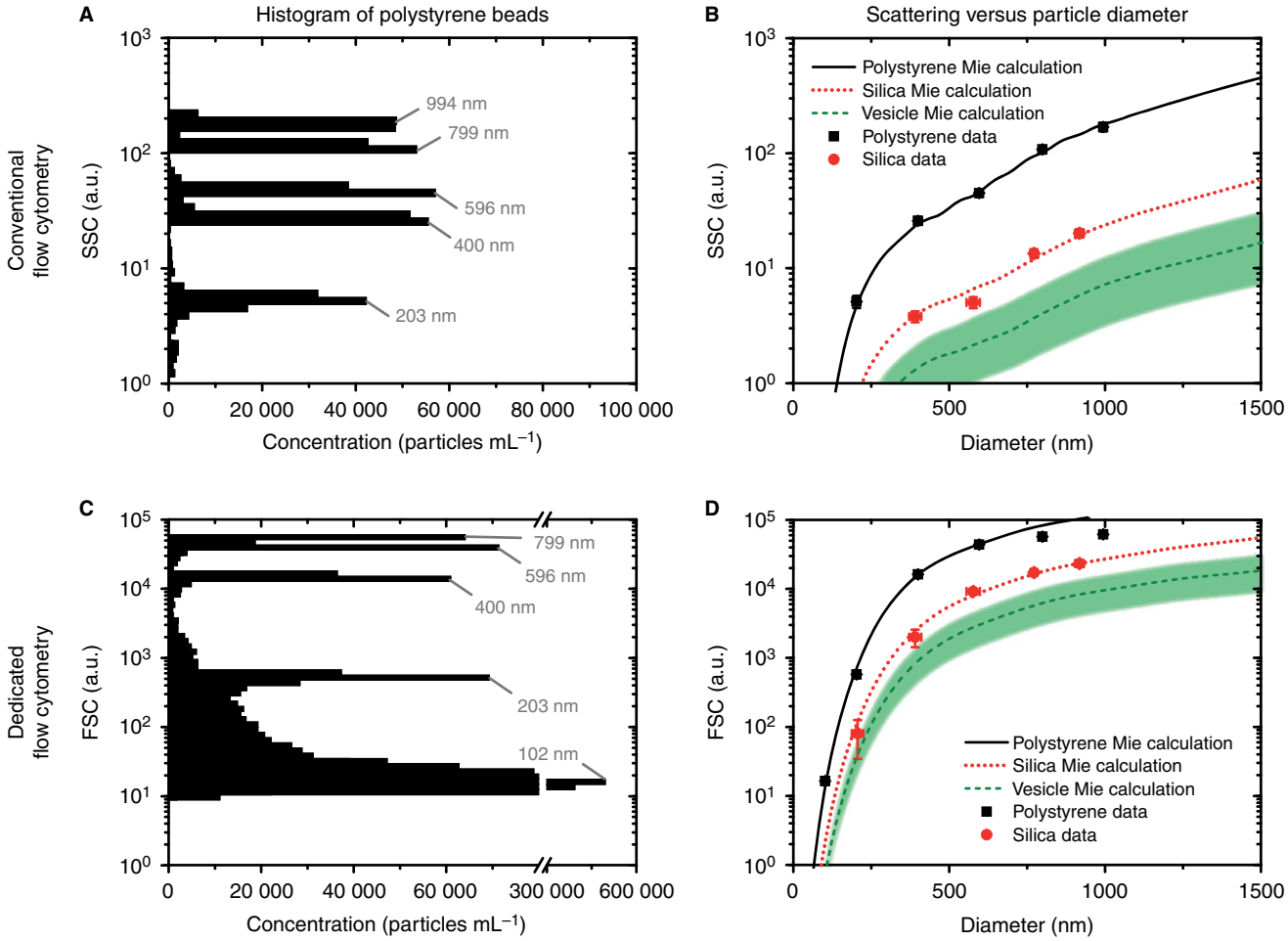

Fig. 2. Relationship between scattering and the diameter of vesicles. (A) Side-scattered light (SSC; logarithmic scale) vs. concentration for polystyrene beads measured by conventional flow cytometry. (B) Measured (symbols) and calculated (lines) SSC (logarithmic scale) vs. diameter for polystyrene beads (black), silica beads (red), and vesicles (green). The SSC increases with increasing particle diameter, and is lower for vesicles than for beads. (C) Forward-scattered light (FSC; logarithmic scale) vs. concentration for polystyrene beads measured by dedicated flow cytometry. The concentration of 102-nm beads was 100-fold higher than that of the other sizes to discriminate between signal and background counts. (D) Measured (symbols) and calculated (lines) FSC (logarithmic scale) vs. diameter for polystyrene beads (black), silica beads (red), and vesicles (green). Mie calculations are in excellent agreement with the data, except for the 799-nm and 994-nm polystyrene beads, owing to detector saturation. a.u., arbitrary units.

sample volume depends on the pore size. With the NP100 pore, only 0.9 nL of sample was analyzed, containing < 1 bead of 596 nm on average. With the NP400 pore, 80 nL was analyzed, containing 77 beads of 596 nm.

The reference beads were analyzed by RPS with high-sensitivity settings (NP100; voltage, 0.70 V; stretch, 47.0 mm) and low-sensitivity settings (NP400; voltage, 0.26 V; stretch, 46.5 mm). The vesicle standard was diluted 1 : 1, and analyzed with high-sensitivity settings (NP100; voltage, 0.60 V; stretch, 46.0 mm) and low-sensitivity settings (NP400; voltage, 0.40 V; stretch, 43.5 mm). The pressure was set at 7.0 mbar. Calibration was performed with beads supplied by the manufacturer. At least 1000 particles per sample were analyzed. A custom-made Microsoft Visual Basic 2008 application interrupted the measurement when the root-mean-square noise exceeded 10 pA. We required the R^2-correlation of cumulative counts with time to exceed 0.999, and the baseline current drift not to exceed 5%. The two PSDs are combined in a similar way as for NTA.

Results

TEM

Figure 1 shows all PSDs of the reference beads and vesicle standard. Figure 1A shows the reference bead PSD based on the prepared concentrations and manufacturer-supplied data. Figure 1B shows the vesicle standard PSD measured by TEM. The combined PSD has a peak at 45 nm, and for larger vesicles the concentration decreases with increasing size. The spikes on the right-hand side correspond to single vesicles. TEM can detect the smallest vesicles present, owing to an imaging resolution of

~ 1 nm. However, sample preparation may cause a reduction in vesicle size [18,24,25]. In addition, limited and non-uniform adhesion of vesicles on the surface may affect the PSD.

Conventional flow cytometry

Figure 1C shows that the smallest polystyrene bead detected by conventional flow cytometry was 203 nm, and that the peaks were broadened as compared with the reference bead PSD. Figure 1D shows that the first bin of the vesicle standard PSD corresponds to 340 nm, which is 140 nm larger than the smallest detected polystyrene bead, owing to refractive index differences. The detected concentration was 1.8×10^7 vesicles mL^{-1}.

Dedicated flow cytometry

Dedicated flow cytometry is capable of detecting single 102-nm polystyrene beads, as shown in Fig. 1E. The width of the peaks is comparable to the reference bead PSD. Figure 1F shows that the first bin of the vesicle standard PSD corresponds to 160 nm. Consequently, dedicated flow cytometry detected approximately twice as small and thereby 18-fold more vesicles than conventional flow cytometry. The detected concentration was 3.3×10^8 vesicles mL^{-1}. Figure 1D,F was produced on the assumption of a vesicle refractive index of 1.40 [14,21,22].

NTA

Figure 1G shows the reference bead PSD as detected by NTA. By combining two measurements with different settings, NTA detected all reference bead sizes, although only 5% of the 46-nm beads were detected. Tracking of 46-nm beads was hindered by the presence of larger beads that saturated the camera. Figure 1G also shows that the peaks overlap because of broadening, which we attribute to the uncertainty in the measured diffusion coefficient, resulting from a limited track length and the uncertainty in the particle position. Figure 1H shows the vesicle standard PSD obtained by combining two different settings. The peak at 95 nm is broad as compared with other vesicle PSDs. The smallest detectable vesicles appear to be 10 nm, which we attribute to broadening of the PSD. Using identical settings, we could detect only 5% of the 46-nm polystyrene beads, which have comparable light scattering to a 70–90-nm vesicle.

RPS

Figure 1I shows the reference bead PSD as detected by RPS. Through combination of measurements with an NP100 and NP400 pore, beads of 102 nm and larger were detected. The peaks are broadened as compared with the reference bead PSD, which may be caused by particle aggregation, electronic noise, and a varying pore dimension during the measurement. Figure 1J shows the vesicle standard PSD with a peak at 75 nm.

Power-law function to describe the PSD of vesicles

The PSDs of vesicles are fitted by a mathematical function to enable quantitative comparison. To select the most appropriate function, we fitted the vesicle standard PSD with six empirical functions that are frequently used to describe PSDs of particles in suspension [16], and performed goodness-of-fit tests (Data S1). The Gamma function, Weibull distribution and power-law function resulted in the best fits. Of these functions, we selected the power-law function, as it is least susceptible to minimum detectable vesicle size. The right panels of Fig. 1 show PSDs of the vesicle standards fitted by the power-law function (dashed lines).

Measurement error and coefficient of variation (CV) of the reference beads

The measured reference bead PSDs in Fig. 1 were fitted by a sum of Gaussian functions (dotted lines) to derive the mean and standard deviation of the size and the concentration for each subpopulation of beads (Table 1). The symbols in Fig. 3A indicate the relative measurement error of the size as the percentage difference between the measurement and the manufacturer specification. Because TEM data were used as reference, its relative size error is set at 0%. The relative size error of the other methods was < 9%. Dedicated flow cytometry had the lowest error in sizing beads, followed by RPS, conventional flow cytometry, and NTA. We attribute the low error of flow cytometry to the homogeneous refractive index of polystyrene and the strong relationship between size and scattering power (Fig. 2). The error of RPS was limited because of specific measurement restrictions, as described in Materials and methods. We attribute the relatively large error of NTA to the uncertainty in the measured diffusion coefficient.

The error bars in Fig. 3A indicate the CV, which is the percentage ratio between the standard deviation and the mean size, and is thus a measure of the width of the peaks in Fig. 1. Owing to the high resolution of TEM as compared with the measured standard deviation of the bead sizes, this standard deviation is a close approximation of the actual size of the beads. The lowest CVs were obtained by dedicated flow cytometry, followed by conventional flow cytometry, RPS, and NTA.

Figure 3B shows the relative measurement error in determining the concentration of subpopulations of reference beads. RPS was most accurate in determining the concentration of beads, followed by conventional flow cytometry, dedicated flow cytometry, and NTA. The error of RPS was limited because of specific measurement

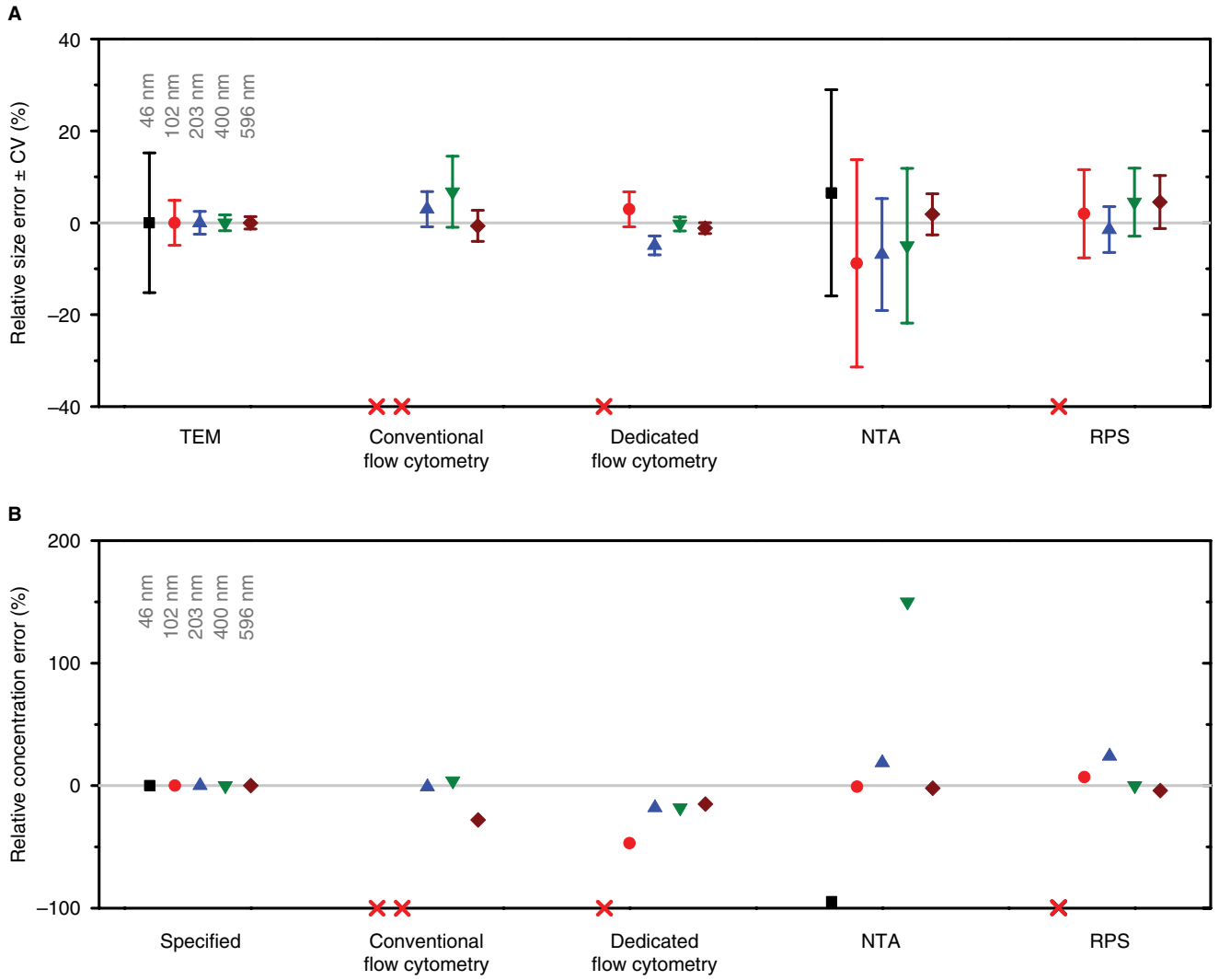

Fig. 3. Relative error (symbols) and coefficient of variation (CV) (error bars) in determining the size (A) and concentration (B) of TEM, conventional flow cytometry, dedicated flow cytometry, nanoparticle tracking analysis (NTA) and resistive pulse sensing (RPS) for 46-nm beads (black), 102-nm beads (red), 203-nm beads (blue), 400-nm beads (green) and 596-nm beads (brown) from the reference mixture. Subpopulations that could not be detected are indicated by red crosses.

restrictions. With flow cytometry, the concentration was derived from the flow rate, which has an uncertainty of 10%. Dedicated flow cytometry underestimated the concentration of 102-nm beads, as these beads were close to the detection threshold. NTA was the least accurate method for determining the concentration of beads, possibly because of broadening of the PSD and crosstalk between 203-nm beads and 400-nm beads. The concentration of 46-nm beads was underestimated, as tracking of 46-nm beads was hindered by the presence of larger beads that saturated the camera.

Concentration of vesicles

Figure 4 shows the detected concentration of vesicles per technique. As compared with RPS and NTA, conventional flow cytometry underestimates the concentration of vesicles almost 300-fold, whereas the more sensitive dedicated flow cytometer underestimates the vesicle concentration 15-fold. With TEM, the detected concentration was affected by sample preparation losses.

Discussion and conclusion

In this study, we compared the abilities of five commonly used methods to determine the PSD of vesicles in suspension. A reference mixture of polystyrene beads with known PSD (Fig. 1A) and a vesicle standard from urine (Fig. 1B) were measured by each method. In agreement with our theoretical review [9], each technique gives a different PSD for the same sample. By comparing the vesicle PSDs and combining these results with the knowledge obtained from reference beads, however, many differences are now explained.

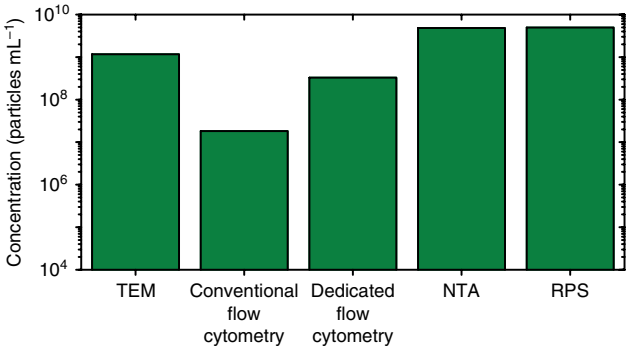

Fig. 4. Total detected concentration (logarithmic scale) of vesicles detected by transmission electron microscopy (TEM), conventional flow cytometry, dedicated flow cytometry, nanoparticle tracking analysis (NTA), and resistive pulse sensing (RPS).

Throughout the Results section, we have discussed the requirements and assumptions involved in the measured PSDs. Table 3 summarizes these requirements and assumptions, and also lists the minimum detectable vesicle size, the measurement times, and the capabilities to obtain functional information, such as fluorescence. In the next section, we will discuss our approach and the results in more detail.

TEM

To obtain the size of the reference beads (Fig. 1A), we used traceable TEM measurements of the manufacturer. Traceability means that the measurement result is related to SI units through an unbroken chain of comparisons with known uncertainties [26,27]. To characterize beads, TEM is particularly useful, as beads are not affected by sample preparation, and the resolution of TEM is higher than the size of the beads. For comparison purposes, we set the relative size error of TEM to 0 (Fig. 3A). However, the relative size error of the reference beads ranges from 1.0% for the 596-nm beads to 4.3% for the 46-nm beads. The TEM data also provide the CV of the beads, which is a measure of the spread in bead sizes. Consequently, the error bars in Fig. 3A represent not only the imprecision of the instrument, i.e. the broadening of the reference bead PSD caused by the instrument, but also the CV of the reference beads.

We derived the reference bead concentrations from the manufacturer-specified mass concentration, density and size of the beads. Note that the concentration of submicrometer beads is not traceable, as uncertainties in the mass concentration and density of the beads are unknown. The mass concentration is often provided with single-digit precision, and the density of silica beads may range from 1.8 to 2.5 g cm^{-3}. Consequently, the bead concentration and error thereof are unknown, and the relative concentration errors can only be mutually compared (Fig. 3B).

TEM analysis of vesicles involves two centrifugation steps and extensive sample preparation. To quantify the influence of these preanalytic variables on the obtained PSD (Fig. 1B), we overlapped the power-law functions of TEM and RPS, which required horizontal and vertical stretching of the RPS data with factors of 0.88 and 0.21, respectively. Considering RPS to be the most reliable method for determining the PSD of vesicles, we hypothesize that vesicles shrink by 12%, owing to fixation and dehydration, and that 21% of the vesicles are recovered after centrifugation and binding to the formvar coating.

Table 3 Assessed capabilities of techniques for the detection of single vesicles in suspension

Method	Minimum detectable vesicle size (nm)	Size requirements and/or assumptions	Concentration requirements and/or assumptions	Additional features	Measurement time
TEM	~ 1	No shrinkage Equivalent circular size	100% surface binding No centrifugation losses	Immunogold labeling	H
Conventional flow cytometry	270–600	Calibration with beads Spherical particle, $n = 1.40 \pm 0.02$	Q	Fluorescence	S
Dedicated flow cytometry	150–190	Calibration with beads Spherical particle, $n = 1.40 \pm 0.02$	Q	Fluorescence	S
NTA	70–90	T, η, ΔD Spherical particle	Calibration with beads $I_v(d,n) = I_b$	Zeta potential Fluorescence	M
RPS	70–100	Calibration with beads Spherical particle, $\sigma_v \ll \sigma_m$	Calibration with beads Q dominated by Q_P	Zeta potential	M

NTA, nanoparticle tracking analysis; RPS, resistive pulse sensing; TEM, transmission electron microscopy. For each technique, the minimum detectable vesicle size, ability to measure the size and concentration and the requirements for this, ability to detect additional features, and measurement time are estimated. We derived the minimum detectable vesicle size of RPS from six measurements performed with different NP100 pores. d is the vesicle diameter, ΔD is the uncertainty in the diffusion coefficient, I_v and I_b are the scattering intensities of a vesicle and a calibration bead, respectively, η is the viscosity of the solvent, n is the vesicle refractive index, Q is the flow rate, Q_P is the flow rate caused by external pressure, σ_v are σ_m are the electrical conductivities of a vesicle and the medium, respectively, and T is the temperature of the solvent. The measurement time is indicated by S, M, and H, meaning < 1 min, between 1 min and 1 h, and > 1 h, respectively.

Flow cytometry

To relate the measured light scattering to a particle size, we calibrated flow cytometers by using beads and Mie theory (Fig. 2), assuming spherical particles of known refractive index. As beads meet these criteria, Mie theory can be used to determine their PSD (Fig. 1C,E), resulting in dedicated flow cytometry being the most accurate in sizing beads (Fig. 3A). However, the refractive index of vesicles is probably heterogeneous and not exactly known [28], thereby affecting the PSD of vesicles obtained by flow cytometry (Fig. 1D,F). For example, under the assumption that the vesicle refractive index is 1.40 ± 0.02, the minimum detectable vesicle sizes are 270–600 nm for conventional flow cytometry and 150–190 nm for dedicated flow cytometry (Table 3). We attribute the high concentration of vesicles > 340 nm obtained by conventional flow cytometry relative to other techniques to background counts. An advantage of flow cytometry is knowledge of the analyzed sample volume, such that the particle concentration can be determined without calibration with beads.

NTA

The PSD of beads determined by NTA shows extensive broadening as compared with the other techniques (Figs. 1G and 3A). In addition, the determined concentration of vesicles requires careful interpretation. The manufacturer or user calibrates the instrument with beads to relate the mean number of scatterers in the field-of-view to the concentration [23]. This calibration is valid for a vesicle size that scatters the same amount of light as the calibration beads. The concentration of smaller vesicles is underestimated, whereas the concentration of larger vesicles is overestimated. Moreover, the concentration of beads is not traceable. To obtain the minimum detectable vesicle size of 70–90 nm, we related the scattering of 46-nm polystyrene beads, which were at the limit of detection, to the diameter of vesicles by using Mie theory.

Software often applies unknown and undesired operations to the data. For example, Fig. 5 shows the reference bead PSD detected by NTA with the low-sensitivity settings and processed by NTA v2.3.5.16 (Nanosight). Analysis of the videos with this newer software results in a PSD (blue line) different from that in Fig. 1G (blue line). The software generates a batch summary file, wherein a rolling average is applied to the raw data, resulting in a smoother but less correct representation of the data (gray line). Application of finite track length adjustment (FTLA) results in narrower peaks, a decreased accuracy of the determined mean diameters, and the presence of an additional peak at 445 nm (brown line). As FTLA introduces artefacts, the application of FTLA to polydisperse samples is not recommended.

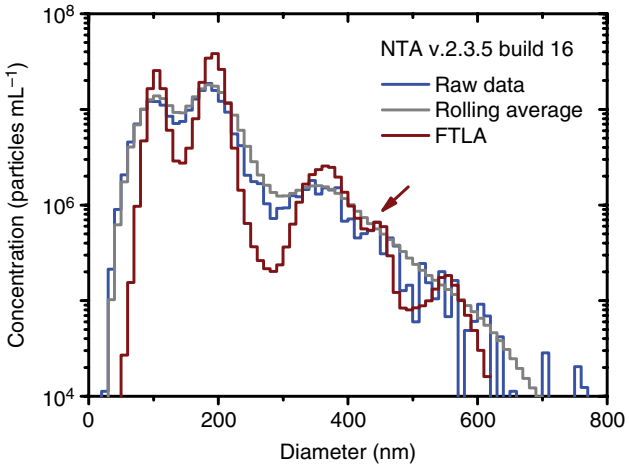

Fig. 5. Particle size distribution (PSD) of the reference beads detected by nanoparticle tracking analysis (NTA) with low-sensitivity settings and processed by NTA v2.3.5.16 software (Nanosight). The bin width is 10 nm. The software provides raw data (blue line), a rolling average of the data (gray line), and data processed with the finite track length adjustment (FTLA) algorithm (brown line), resulting in different PSDs. The FTLA algorithm results in a peak (brown arrow) that is absent in the rolling average of the data.

RPS

Accurate sizing of vesicles by RPS requires that the electrical conductivity of a particle is negligible as compared with the conductivity of the electrolyte [16,29]. As polystyrene beads, cells and intact vesicles meet this requirement [30], we believe that the detected vesicle size is representative for urinary vesicles (Fig. 1J). However, our measurement restrictions made the RPS measurements impractical. The major concerns with RPS are pore clogging and pore stability. In the case of pore clogging, we reversed the pressure or temporarily applied a high pressure with a plunger. As the pores are stretchable, plunging may change the pore dimensions, as observed by a change in the baseline current. If the baseline current changed by > 5%, we repeated the measurement and calibration, resulting in a measurement time of several hours.

The concentration is obtained by calibration with beads [29], which is inaccurate, because the concentration of used beads is not traceable. As the flow rate is mainly determined by pressure across the pore, and not by electro-osmosis or electrophoresis, the differences between the zeta potentials of vesicles and calibration beads are negligible. Consequently, the accuracy in determining the vesicle concentration is expected to be comparable to that for the mixture of beads.

Single-vesicle detection as a biomarker

A biomarker based on vesicle enumeration should determine the concentration of a specific vesicle type. For this determination, the technique must obtain biochemical

information to identify specific vesicles, and the measurement time should not exceed several minutes. Furthermore, size accuracy and precision are important, e.g. to distinguish vesicles from platelets. Our findings demonstrate that any reported concentration needs to be accompanied by the minimum detectable vesicle size. For example, the shaded area in Fig. 1J shows that a decrease in the minimum detectable vesicle size from 80 nm to 60 nm would result in a 2.4-fold increase in the obtained concentration. Therefore, we propose daily monitoring of the minimum detectable vesicle size, as day-to-day variation is expected for each instrument. Alternatively, a power-law fit may be applied to compare concentrations obtained with different minimum detectable vesicle sizes. An additional requirement for comparison of concentrations is traceable determination of both size and concentration, which is problematic for techniques that calibrate the concentration with untraceable beads.

In conclusion, each technique gave a different PSD for the same vesicle sample. Differences between the detected vesicle concentrations are primarily caused by differences between the minimum detectable vesicle sizes. The minimum detectable vesicle sizes were 70–90 nm for NTA, 70–100 nm for RPS, 150–190 nm for dedicated flow cytometry, and 270–600 nm for conventional flow cytometry. TEM could detect the smallest vesicles present, albeit after adhesion on a surface. Dedicated flow cytometry was most accurate in determining the size of reference beads, but is expected to be less accurate on vesicles, owing to heterogeneity of the refractive index of vesicles. A reliable estimate of the vesicle refractive index is required to convert the optical scatter signal detected by flow cytometry to size. Nevertheless, dedicated flow cytometry is relatively fast and allows multiplex fluorescence detection, making it most applicable to clinical research.

Addendum

E. van der Pol, R. Nieuwland, and T. G. van Leeuwen conceived and designed the research. E. van der Pol and A. E. Grootemaat acquired the data. C. Gardiner, E. van der Pol, F. A. Coumans, R. Nieuwland, and T. G. van Leeuwen interpreted the data. E. van der Pol, F. A. Coumans, and R. Nieuwland wrote the manuscript. All authors reviewed and made critical revisions to the manuscript.

Acknowledgements

The authors would like to acknowledge E. van der Pol, Wageningen University, the Netherlands, for statistical support. Part of this work was funded by the EMRP (European Metrology Research Programme) under the Joint Research Project HLT02 (www.metves.eu). The EMRP is jointly funded by the EMRP participating countries within the European Association of National Metrology Institutes and the European Union.

Disclosure of Conflict of Interests

The authors state that they have no conflict of interest.

Supporting Information

Additional Supporting Information may be found in the online version of this article:

Data S1. Methods and mathematical function to fit the particle size distribution of vesicles.

References

1 Conde-Vancells J, Rodriguez-Suarez E, Embade N, Gil D, Matthiesen R, Valle M, Elortza F, Lu SC, Mato JM, Falcon-Perez JM. Characterization and comprehensive proteome profiling of exosomes secreted by hepatocytes. *J Proteome Res* 2008; **7**: 5157–66.

2 Ratajczak J, Wysoczynski M, Hayek F, Janowska-Wieczorek A, Ratajczak MZ. Membrane-derived microvesicles: important and underappreciated mediators of cell-to-cell communication. *Leukemia* 2006; **20**: 1487–95.

3 Simons M, Raposo G. Exosomes – vesicular carriers for intercellular communication. *Curr Opin Cell Biol* 2009; **21**: 575–81.

4 van der Pol E, Böing AN, Harrison P, Sturk A, Nieuwland R. Classification, functions and clinical relevance of extracellular vesicles. *Pharmacol Rev* 2012; **64**: 676–705.

5 Berckmans RJ, Sturk A, Schaap MC, Nieuwland R. Cell-derived vesicles exposing coagulant tissue factor in saliva. *Blood* 2011; **117**: 3172–80.

6 Manly DA, Wang JG, Glover SL, Kasthuri R, Liebman HA, Key NS, Mackman N. Increased microparticle tissue factor activity in cancer patients with venous thromboembolism. *Thromb Res* 2010; **125**: 511–12.

7 Rautou PE, Leroyer AS, Ramkhelawon B, Devue C, Duflaut D, Vion AC, Nalbone G, Castier Y, Leseche G, Lehoux S, Tedgui A, Boulanger CM. Microparticles from human atherosclerotic plaques promote endothelial ICAM-1-dependent monocyte adhesion and transendothelial migration. *Circ Res* 2011; **108**: 335–43.

8 EL Andaloussi S, Maeger I, Breakefield XO, Wood MJA. Extracellular vesicles: biology and emerging therapeutic opportunities. *Nat Rev Drug Discovery* 2013; **12**: 348–58.

9 van der Pol E, Hoekstra AG, Sturk A, Otto C, van Leeuwen TG, Nieuwland R. Optical and non-optical methods for detection and characterization of microparticles and exosomes. *J Thromb Haemost* 2010; **8**: 2596–607.

10 van der Pol E, Coumans F, Varga Z, Krumrey M, Nieuwland R. Innovation in detection of microparticles and exosomes. *J Thromb Haemost* 2013; **11**: 36–45.

11 de Vrij J, Maas SL, van Nispen M, Sena-Esteves M, Limpens RW, Koster AJ, Leenstra S, Lamfers ML, Broekman ML. Quantification of nanosized extracellular membrane vesicles with scanning ion occlusion sensing. *Nanomedicine* 2013; 1–16.

12 Dragovic RA, Gardiner C, Brooks AS, Tannetta DS, Ferguson DJP, Hole P, Carr B, Redman CWG, Harris AL, Dobson PJ, Harrison P, Sargent IL. Sizing and phenotyping of cellular vesicles using nanoparticle tracking analysis. *Nanomedicine* 2011; **7**: 780–8.

13 Yuana Y, Oosterkamp TH, Bahatyrova S, Ashcroft B, Garcia RP, Bertina RM, Osanto S. Atomic force microscopy: a novel

approach to the detection of nanosized blood microparticles. *J Thromb Haemost* 2010; **8**: 315–23.
14 Konokhova AI, Yurkin MA, Moskalensky AE, Chernyshev AV, Tsvetovskaya GA, Chikova ED, Maltsev VP. Light-scattering flow cytometry for identification and characterization of blood microparticles. *J Biomed Opt* 2012; **17**: 0570061–8.
15 van der Pol E, van Gemert MJC, Sturk A, Nieuwland R, van Leeuwen TG. Single versus swarm detection of microparticles and exosomes by flow cytometry. *J Thromb Haemost* 2012; **10**: 919–30.
16 Jonasz M, Fournier GR. *Light Scattering by Particles in Water*, 1st edn. London: Academic Press, 2007.
17 Nieuwland R, van der Pol E, Gardiner C, Sturk A. Platelet-derived microparticles. In: Michelson AD, ed. *Platelets*, 3rd edn. San Diego, CA: Academic Press, 2012: 453–67.
18 Yuana Y, Bertina RM, Osanto S. Pre-analytical and analytical issues in the analysis of blood microparticles. *Thromb Haemost* 2011; **105**: 396–408.
19 Bohren CF, Huffman DR. *Absorption and Scattering of Light by Small Particles*. New York, NY: Wiley, 1983.
20 Mätzler C. MATLAB functions for Mie scattering and absorption. 2002–11. 2002. Institut für Angewandte Physik.
21 van Manen HJ, Verkuijlen P, Wittendorp P, Subramaniam V, van den Berg TK, Roos D, Otto C. Refractive index sensing of green fluorescent proteins in living cells using fluorescence lifetime imaging microscopy. *Biophys J* 2008; **94**: L67–9.
22 Beuthan J, Minet O, Helfmann J, Herrig M, Muller G. The spatial variation of the refractive index in biological cells. *Phys Med Biol* 1996; **41**: 369–82.
23 Gardiner C, Ferreira YJ, Dragovic RA, Redman CWG, Sargent IL. Extracellular vesicle sizing and enumeration by nanoparticle tracking analysis. *J Extracell Vesicles* 2013; **2**: 1–11.
24 Théry C, Amigorena S, Raposo G, Clayton A. Isolation and characterization of exosomes from cell culture supernatants and biological fluids. *Curr Protoc Cell Biol* 2006; **30**: 3.22.1–22.29.
25 Jensen OA, Prause JU, Laursen H. Shrinkage in preparatory steps for SEM – a study on rabbit corneal endothelium. *Albrecht Von Graefes Arch Klin Exp Ophthalmol* 1981; **215**: 233–42.
26 Meli F, Klein T, Buhr E, Frase CG, Gleber G, Krumrey M, Duta A, Duta S, Korpelainen V, Bellotti R, Picotto GB, Boyd RD, Cuenat A. Traceable size determination of nanoparticles, a comparison among European metrology institutes. *Meas Sci Technol* 2012; **23**: 125005.
27 Varga Z, Yuana Y, Grootemaat AE, van der Pol E, Gollwitzer C, Krumrey M, Nieuwland R. Towards traceable size determination of extracellular vesicles. *J Extracell Vesicles* 2014; **3**: 1–10.
28 Issman L, Brenner B, Talmon Y, Aharon A. Cryogenic transmission electron microscopy nanostructural study of shed microparticles. *PLoS One* 2013; **8**: e83680.
29 Kachel V. Electrical resistance pulse sizing: Coulter sizing. In: Hoffman RA, ed. *Flow Cytometry and Sorting*, 2nd edn. New York, NY: Wiley-Liss, 1990: 45–80.
30 Montesinos E, Esteve I, Guerrero R. Comparison between direct methods for determination of microbial cell-volume – electron-microscopy and electronic particle sizing. *Appl Environ Microbiol* 1983; **45**: 1651–8.